Materials and Design 198 (2021) 109327

Contents lists available at ScienceDirect

Materials and Design

journal homepage: www.elsevier.com/locate/matdes

Mechanism of chip formation and surface-defects in orthogonal cutting of soft-brittle potassium dihydrogen phosphate crystals

Qi Liu [a,b], Zhirong Liao [b,*], Jian Cheng [a], Dongdong Xu [b], Mingjun Chen [a,*]

[a] State Key Laboratory of Robotics and System, Harbin Institute of Technology, Harbin 150001, China
[b] Machining and Condition Monitoring Group, Faculty of Engineering, University of Nottingham, Nottingham NG7 2RD, UK

HIGHLIGHTS

- Chip formation mechanism and surface-defects in orthogonal cutting of KDP has been studied.
- The change of cutting modes (e.g., plastic, shear-crack,fracture modes) depends on the value of uncut chip thickness.
- A theoretical model model regarding energy release rate was proposed to clarify the transition mechanism of cutting modes.
- Micro pits, cracks, and edge chippings are the three types of surface defects that occurred on machined surfaces.

GRAPHICAL ABSTRACT

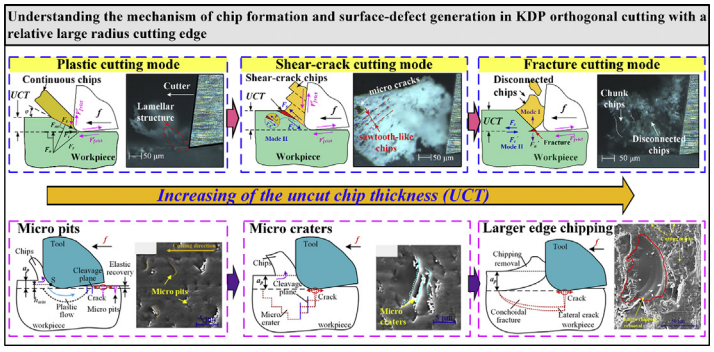

ARTICLE INFO

Article history:
Received 17 August 2020
Received in revised form 6 November 2020
Accepted 11 November 2020
Available online 13 November 2020

Keywords:
Soft-brittle KDP crystals
Orthogonal cutting
Chip formation
Material removal mechanism
Brittle-to-ductile transition

ABSTRACT

Micromachining repair of surface defects on KH_2PO_4 (KDP) optics is an emerging technique in the construction of Inertial Confinement Fusion facilities for obtaining clean nuclear fusion energy. However, this method is yet facing considerable challenges owing to the soft-brittle nature of single-crystal KDP, hence it is necessary to understand its ductile-regime cutting mechanism to generate crack-free surfaces. This paper seeks to investigate the evolution of different cutting mechanism with the change of uncut chip thickness (UCT) in KDP orthogonal cutting processes. A transition of cutting modes from plastic cutting to shear-crack cutting and then fracture cutting with the rise of UCT has been revealed. To explain these cutting phenomena, a novel theoretical model was proposed by calculating the specific energy dissipation for crack/fracture propagations during cutting processes based on fracture mechanics. This analytical model was well validated by the analysis of cutting forces and machined surface quality. Nevertheless, three kinds of surface defects have been observed, i.e. micro pits, micro craters and edge chipping. These surface defects were caused by tearing and spalling of materials with elastic recovery, crack propagation along cleavage planes with ploughing effect, and the peeling away of large-size fracture, respectively. The presented results of great significance for promoting the application of micromachining processes in future engineering repair of KDP optics.

1. Introduction

Soft-brittle optical crystals, like potassium dihydrogen phosphate (KH_2PO_4/KDP), are extensively employed in the construction of Inertial Confinement Fusion (ICF) facilities [1,2]. However, in the practical ultra-precision manufacturing (i.e. single-point diamond turning, SPDT) and

* Corresponding authors.
E-mail addresses: Zhirong.Liao@nottingham.ac.uk (Z. Liao), chenmj@hit.edu.cn (M. Chen).

https://doi.org/10.1016/j.matdes.2020.109327

laser irradiation processes, these KDP optical components are susceptible to generate some surface defects such as micro-cracks, which could cause severe laser-induced damage and significantly deteriorate the ultimate optical performance of KDP optics [3]. Hence, in order to reuse and recycle these expensive optical components, the most cost-effective method is to mitigate and repair these optics as soon as any micro defects occur. Currently, the micro-milling approach has been proposed as the most promising technique for mitigating those original defects on KDP surfaces with predesigned smooth three-dimensional (3D) contours [4,5]. However, owing to the specific soft-brittle natures of KDP materials, it is a real challenging task to achieve a smooth repaired surface without any cracks because the cutting edge radius (r_e) adopted in practical milling repair processes is around 1 μm [6], distinct to that (<100 nm) in SPDT process [7]. Considering the geometric of cutting tool exerts a significant role in the brittle-to-ductile transition (BDT) of cutting modes when manufacturing brittle materials [8], the material removal behaviour cut by a relatively large-radius cutting edge must differ from that by a sharp cutting edge (e.g., SPDT), especially in the machining of soft-brittle materials. Therefore, figuring out the material removal and surface formation mechanism with a relatively large-radius cutting edge is of great importance in optimizing cutting conditions and tool design for enhancing the repair quality and also improving the ultimate optical performance of repaired KDP optics.

In the research of SPDT of KDP crystals, considerable efforts have been made to investigate the ductile-regime machining mechanism. It was revealed that the brittle-to-ductile transition of cutting modes is highly dependent on the values of UCT [9,10] and a nanoscale UCT is found to be conducive to the formation of hydrostatic compressive pressure underneath the cutting area and thus contribute to the suppression of cracks [11]. This nanoscale material removal volume is exactly the reason why single-point diamond cutters with a sharp cutting edge (<100 nm) are widely adopted in the ultra-precision machining of brittle materials. However, the material removal behaviour in the mechanical repair process of KDP optics is quite different from that in the SPDT process. On the one hand, during the micro-milling process, the instantaneous UCT in one cutter rotation can no longer be regarded as a constant value like that in SPDT as it changes synchronously with the rotation of cutter [12,13]. At the same time, the actual UCT has also been identified to be increased by the elastic recovery behaviours of workpiece materials in micro-milling processes which were caused by previous cutting tooth passes [14,15]. This dynamic chip thickness revolution and accumulation can not only have a vital effect on the cutting forces but also play a role in the material removal behaviours and also the resultant machined surface quality [14]. This influence induced by the dynamic changes of UCT might be more obvious when machining soft-brittle materials like KDP crystals. On the other hand, as mentioned above, a micro ball-end milling cutter with a relatively large-radius cutting edge ($r_e \approx 1$ μm) is adopted in the practical repair processes, which is more economical than diamond micro mills with sharp cutting edges ($r_e < 100$ nm). Recently, smooth Gaussian 3D contours (Ra <38 nm) were produced by Liu with micro-milling cutters ($r_e \approx 1$ μm) [12,16] and the laser-induced damage resistance of these repaired contours were found comparable with that of original KDP optics processed by SPDT. The employed milling cutters are made of non-diamond materials [6] (e.g, cubic boron nitride and cemented carbide), the application of which significantly improves the machinability of soft-brittle KDP crystals and could further reduce the expensive demand for diamond cutters in the engineering repair of KDP optics. Nevertheless, these reported studies are mainly focused on the achievement of ductile-regime surfaces of KDP optics and have not fully uncovered the specific chip formation mechanism when machining this type of soft-brittle crystals with a relatively large-radius cutting edge. Although continuous and broken chips have been observed in SPDT cutting trials [11], the underlying theoretical relationship between the UCT, material removal and surface defects formation has not been fully clarified.

Meanwhile, the orthogonal cutting approach has been widely employed as a powerful method in the mechanical machining field of difficult-to-cut materials to understand their unique cutting mechanism [17,18]. Through this approach, chip formation process can be captured in-situ by advanced cameras to provide adequately direct details for the understanding of specific material removal mechanism within different cutting conditions [19] (i.e., uncut chip thickness, cutting strain-rate). Thus, in-situ observing the chip formation process at different UCT is one of the most important merits of the orthogonal cutting approach. Besides, the specific cutting energy could also be obtained by analysing the cutting forces for guiding the selection of cutting parameters in actual machining processes [17]. Nevertheless, to the best of the author's acknowledge, this approach has been mainly applied in the machining of ductile materials and few efforts have been made to brittle materials. Although the chip formation processes of some brittle materials (i.e. bone [10,20] and Ceramic Matrix Composites [21], CMC for short) have been uncovered recently based on this approach, the revealed mechanism seems not appliable in the machining of KDP crystals. This is because both the bone and CMC are heterogeneous materials and the ductile cutting of these materials can be achieved by selecting a specific cutting direction regarding their material structures and properties [22] while KDP is a unique soft-brittle single-crystal and the ductile cutting is predominated by the actual values of UCT in practical cutting processes which have been reported be less than one micrometre [23]. Therefore, more efforts, i.e. orthogonal cutting trials, are supposed to be performed to reveal the specific cutting mechanism and surface defects formation when machining this type of soft-brittle crystals at different uncut chip thicknesses from the nanoscale to microscale.

The state-of-the-art shows that the problems in the micro-milling repair operations of KDP surface defects have been extensively investigated. It is also proved that non-diamond cutters can be employed to repair KDP optics and could be used in large quantities in the actual repair engineering due to their lower-cost advantages [24]. Nevertheless, the material removal process, especially the chip formation behaviours, at different uncut chip thicknesses has not been fully understood when machining this type of soft-brittle KDP crystals with a relatively large-radius cutting edge. Moreover, the brittle-to-ductile transition (BDT) mechanism during the cutting process keeps still unclear from the view of fracture mechanics. Recently, one fracture criterion was proposed to understand the ductile-regime cutting mechanism of some brittle materials like bone [10,25] by calculating the actual energy release rate in orthogonal cutting processes and could well explain the crack propagation behaviours and BDT mechanism. Therefore, in order to further understand the material removal mechanism of soft-brittle KDP crystals cut by a relatively large-radius cutting edge, a theoretical analysis on the energy release rate is in urgent need to explain the inherent relation between the chip formation and UCT and the resultant formation of surface-defects.

In light of this, this paper is aimed to investigate the specific material cutting mechanism and surface-defect formation in the orthogonal cutting of soft-brittle KDP crystals. Firstly, a serial of orthogonal cutting trials was performed at various UCT and the transition of cutting modes has been identified by observing the chip formation processes. Afterwards, in order to reveal the transition mechanism of different cutting modes, a theoretical approach was proposed to calculate the energy release rate by combining the obtained experimental results and to analyze the various chip formation behaviours at different UCTs. Then, the proposed model was validated experimentally through the analysis of cutting forces and surface morphologies. Besides, the surface defects occurred on the machined surface have also been identified as micro pits, micro craters and edge chipping, and the related formation mechanism was also revealed. This work could provide a valuable understanding of the specific material removal mechanism of soft-brittle single crystals under one non-traditional cutting condition and contribute to the future design of the machining strategies of KDP optics for their engineering repair in ICF facilities.

2. Experimental design and orthogonal cutting details

In order to better achieve the ductile-regime cutting in micro-machining repair processes of soft-brittle KDP crystal, the orthogonal cutting method was employed to explore the material removal mechanism with a relatively large-radius cutting edge similar with that used in micro-milling processes (at micro-scale level). The employed KDP crystal workpiece with a crystallographic orientation of Double plane has been firstly fly-cutting. This Double plane has been widely employed for frequency-doubling conversion in ICF facilities and is known for its difficult-to-machine property [9]. Afterwards, it has been sliced carefully into small blocks with a width of 2 mm by diamond wire saw along [110] direction (Fig. 1) as this direction has been identified to have the largest critical UCT of brittle-to-ductile transition on this plane [9]. In order to meet the plane strain condition of orthogonal cutting in Merchant's theory [26], the sample width was slightly larger than that of the cutting edge (2 mm). All these samples were fine-polished using 4000-grit abrasive papers with denatured alcohol coolant to obtain smooth surfaces for the related micro graphical analysis.

As shown in Fig. 2, the orthogonal cutting tests were performed on a precision four-axis micro milling machine. The detailed information about this experimental setup can be founded in the previous work of Axinte et al., [27]. Meanwhile, a solid carbide cutter with an edge radius (r_e) of 1.118 μm was adopted to simulate the material cutting behaviour in practical micromachining repair processes where the employed mill cutter has a similar size of cutting edge radius [6]. Both the rake angle and flake angle of this cutter are 8°. The UCT was changed from 50 nm to 16 μm within the same feed rate (10 mm/min) since a larger range of UCT and a smaller feed rate are beneficial to understand the cutting mechanism. The detailed experimental parameters used in KDP orthogonal cutting tests are presented in Table 1. All cutting trials were performed under dry cutting conditions. During the cutting process, a 3D VHX Keyence microscopy system was set close to the cutting zone to on-line observe the chip formation morphologies. Meanwhile, a miniature dynamometer (Kistler 9317B) was adopted to measure the cutting forces. After all cutting tests, the obtained surfaces were observed by Scanning Electron Microscopy (Quanta 650) to analyze the formation mechanism of surface defects occurred in KDP cutting process.

3. Analysing and modelling the KDP chip formation behaviours

To study the material removal mechanism of soft-brittle KDP crystals, a serial of orthogonal cutting trials was first conducted with varying UCT to observe the chip formation behaviours and to identify the different cutting modes. Afterwards, a theoretical model would be proposed to calculate the energy release rate by combining the obtained experimental results and to reveal the specific brittle-to-ductile transition mechanism of different cutting modes.

3.1. Chip formation behaviours with different uncut chip thicknesses

Fig. 3 shows the representative chip morphologies formed in KDP orthogonal cutting trials with varying uncut chip thickness (UCT). It was interesting to find that at nano/micro-scale, the chip formation process can be segregated in three modes according to the practical magnitude of UCT. Specifically, for UCT at nano/submicro level (<750 nm), continuous chips are generated while with the increase of UCT (> 1 μm), the chips start to present shear-crack features with a flocculent morphology, and ultimately evolve into fracture form at a large UCT (> 4 μm) which presents disconnected and even powder morphology.

More specifically, as shown in Fig. 3a, when the UCT was less than 100 nm, with the advance of cutting tool, only a few of workpiece materials has generated in front of the cutting area. With the rise of UCT, continuous chips start to form as the result of the plastic shearing deformation (Fig. 3b), similar to the traditional metal-cutting [19,28]. The curly and long chips with flocculence-like morphologies shown in Fig. 3c-d illustrate that a combination of shear and crack behaviours has engaged in the material removal process once the UCT becomes higher than 1 μm. Furthermore, the fractured chips in Fig. 3e and also the powered chips in Fig. 3f jointly demonstrate that the brittle fractures dominate the material removal process at a large UCT (> 4 μm). Hence, three different cutting modes can be concluded during KDP cutting: plastic cutting (UCT < 1 μm), shear-crack cutting (1 μm < UCT < 4 μm) and fracture cutting (UCT > 1 μm). Considering the high brittleness of KDP wherein the brittle-to-ductile transition would occur under different UCT, these phenomena will be explained through theoretical modelling in the following section.

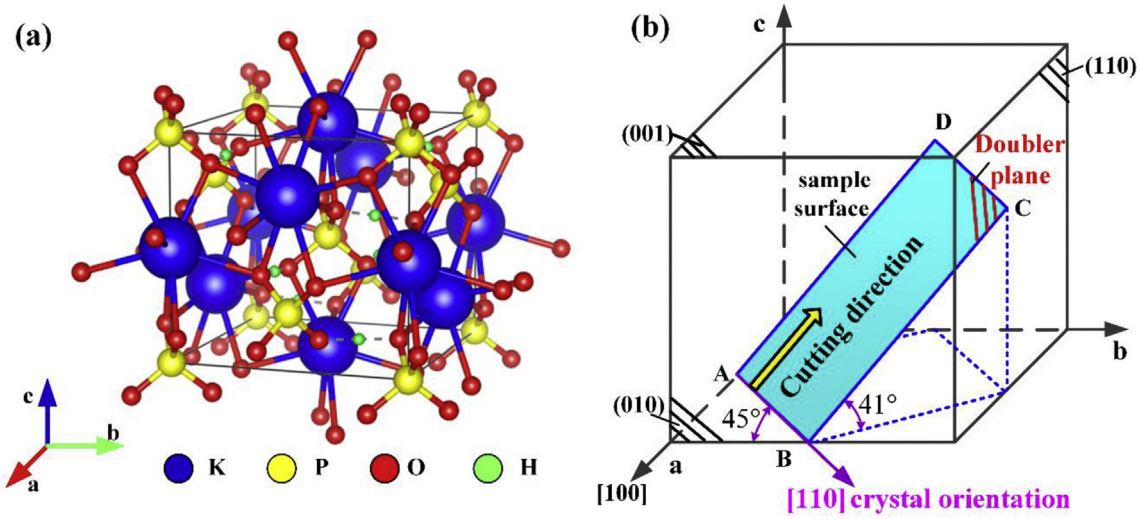

Fig. 1. The 3D crystal structure of single-crystal KDP (a) and the corresponding coordinate system (b). (a) The 3D crystal structure of single-crystal KDP; (b) the corresponding coordinate system showing: the crystal orientation [110] (purple arrow); Doubler plane as sample surface (red lines) [9]; the cutting direction (yellow arrow).

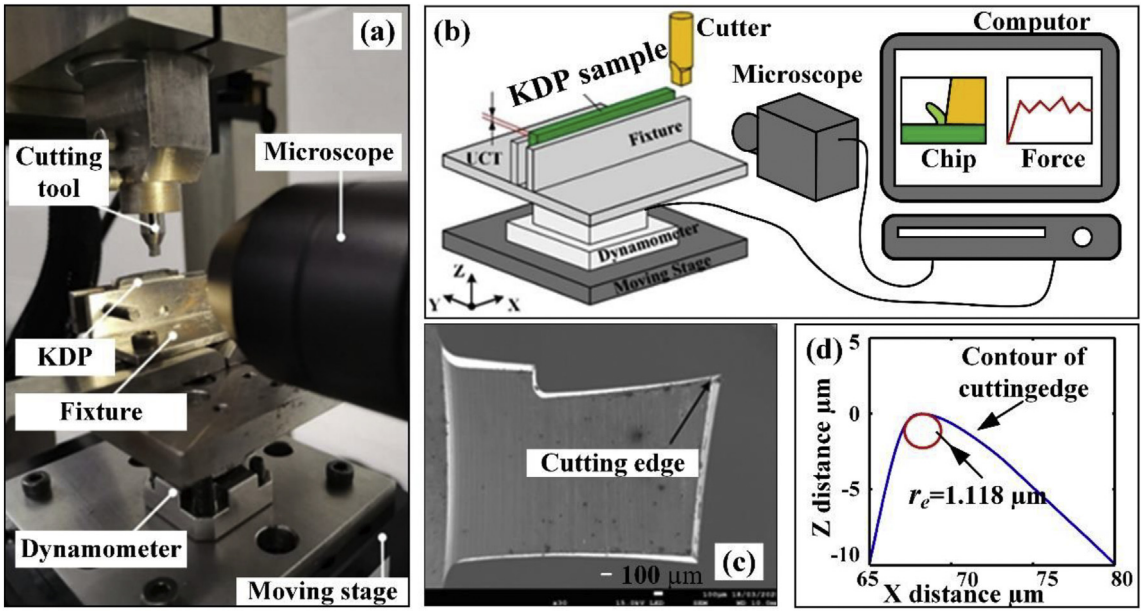

Fig. 2. Images of the orthogonal cutting setup for KDP crystals: (a) Close snapshot of experimental set-up; (b) Schematic of on-line observation of chip formation and cutting forces; (c) SEM images of cutting edge; (d) Measurement of the radius of cutting edge.

Table 1
The parameters used in KDP orthogonal cutting tests.

Parameters	Values
Crystal type	Doubler plane
Feed rate (mm/min)	10
Undeformed cutting depth (μm)	0.1, 0.25, 0.5, 0.75, 1, 1.25, 1.5, 1.75, 2, 3, 4, 6, 8,10, 12,14, 16

3.2. Modelling the chip formation behaviours

As observed in orthogonal cutting processes, the chip formation behaviour in KDP cutting is highly dependent on the magnitude of the UCT, and therefore, the related material removal can be divided into three types according to the values of UCT: (a) plastic cutting mode (PC); (b) shear-crack cutting mode (SCC); (c) facture cutting mode (FC). Furthermore, it was found that the plastic cutting mode under ductile-regime is achieved only within nano/submicro UCT, while the shearing-crack and fracture cutting modes occurs once UCT reaches

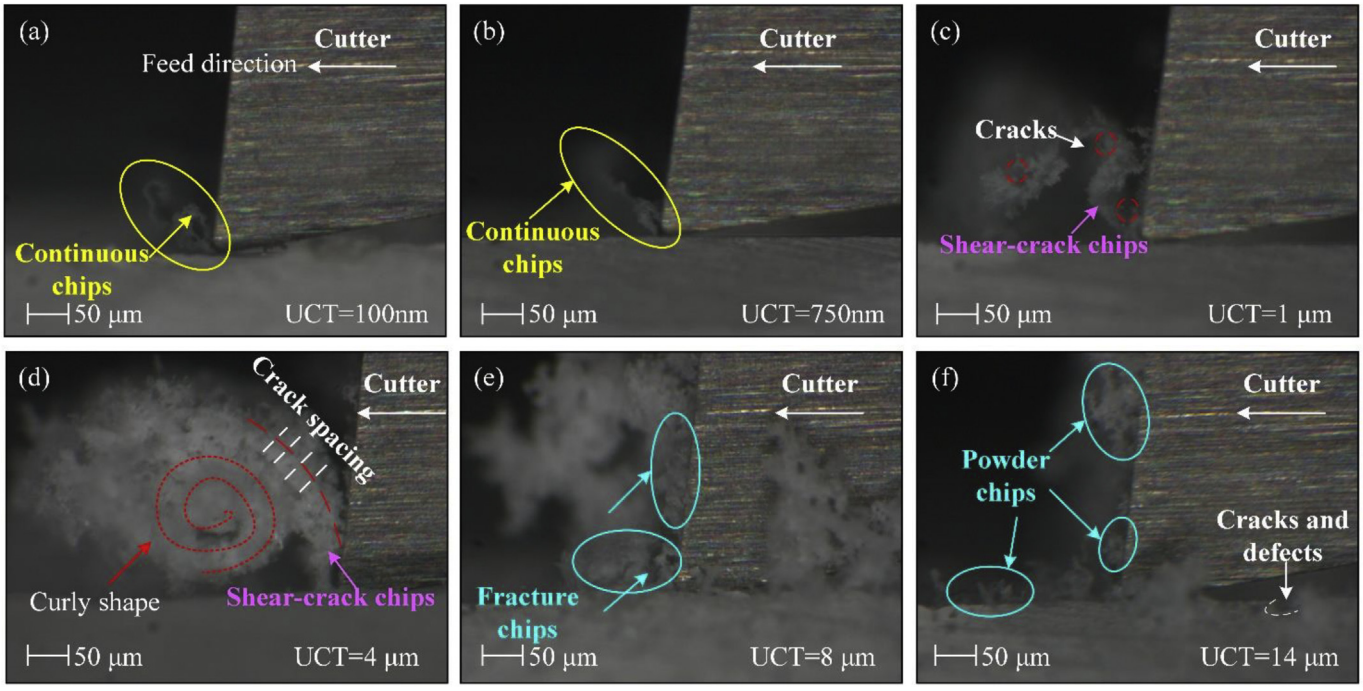

Fig. 3. The evolution of chip morphologies with the increase of UCT shows three different cutting modes: (a) and (b) plastic cutting, (c) and (d) shear-crack cutting, (e) and (f) fracture cutting.

micro-scale level. This is because of the specific properties (e.g. high brittleness, low hardness and low tensile strength) of KDP crystals [29], which pose a great risk of crack generation. Hence, in order to better facilitate the understanding of the material removal mechanism in KDP orthogonal cutting, a novel theoretical analysis based on fracture mechanics is proposed in the following section for revealing the underlying relationship between the cutting modes, UCT, and the energy consumption in the chip formation process.

As validated in the existing literature [10], the brittle crack/fracture failure occurred in orthogonal cutting is the combined behaviour of Mode I and II, as shown in Fig. 4, which are the two main modes of material fracture in fracture mechanics. Thus, the fracture behaviour in KDP orthogonal cutting can be described by energy release rate (G), which characterizes the change in potential energy when the crack grows and the critical value of which represents the amount of energy that is needed to create a crack surface [30].

$$G = -\frac{dU}{dA} = \frac{1}{w}\frac{dU(l)}{dl} \tag{1}$$

where U is the total consumed energy applied by the external forces and internal elastic-strain energy; The terms A, w, l are the crack propagation zone, cutting width and crack length, respectively.

The brittle crack/fracture behaviours occur when the specific energy dissipation rate (G) consumed in the crack zone exceeds the critical threshold called fracture energy (G_c, also named as fracture toughness) at specific cutting-load mode. For instance, the opening crack/fracture which is in the form of Model I would occur once the related energy release rate (G_I) surpasses the theoretical fracture toughness (G_{Ic}): $G_I > G_{Ic}$. During the practical cutting process of brittle materials, Mode I may occur in the cutting direction due to the movement of tool tip while Mode II can occur along shear plane accompanied by extensive shear deformation [10].

In regarding to the KDP cutting, as the consumed energy is mainly provided by the external forces, the energy release rate (G) hence is supposed to have a proportional relation with the practical cutting forces. That is to say, the value of G generally increases with the rise of UCT, and brittle crack failure would take place once the G surpasses the critical value (G_c). Therefore, a theoretical analysis based on fracture mechanic will be developed to investigate the specific cutting mechanism of soft-brittle KDP crystals with different UCTs.

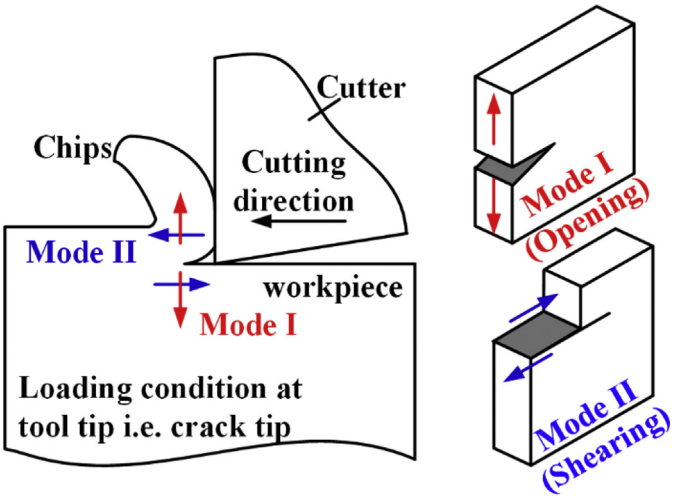

Fig. 4. Schematic of the possible modes of brittle fractures during orthogonal cutting [10].

3.2.1. Analysis of the continuous chip formation in plastic cutting (PC) mode

As revealed in the literature [2,6], the KDP cutting undergoes a significant brittle-to-ductile transition when the UCT decreases down into nano/micro scale although this material is quite brittle in macro scale. Within nano/submicro UCT, the material is mainly removed in form of continuous chips through a plastic cutting (PC) mode (Fig. 3b); hence in this condition, the KDP cutting process can be regarded as in ductile regime. In this case, the detailed material removal process can be explained by adopting Merchant's shear cutting theory [26], in which a shear plane description can be introduced to interpret the deformation behaviour of the material being cut. As illustrated in Fig. 5, within the small UCT, many shear deformation would be generated in the first primary cutting zone caused by the shear force with the advance of cutting tool. As a consequence, continuous chips were generated. This result implies that when cutting within nano/micro UCT the cutting process can be identified in ductile-regime and also demonstrates that the energy released rate (G) in this cutting process is certainly smaller than the critical value (G_c) for crack propagation. Therefore, brittle crack/fracture failure could not be introduced in this case. Meanwhile, due to the shear deformation, a great number of cutting heat would be generated and gradually accumulated adjacent to the shear plane, heightening the plastic capacity of soft-brittle KDP crystals and in return facilitating the plastic cutting behaviour to dominate the chip formation process [2].

3.2.2. Analysis of the shear-crack chip formation in shear-crack cutting (SCC) mode

As shown in Fig. 6a, shear-crack chips have been generated in this mode, accompanied by a large number of micro cracks. The occurrence of these shear-crack morphologies resulted from a combination of both shear and crack behaviours of the material layer being cut ahead of the cutting edge, indicating that the G accumulated in the shear plane due to the deformation surpasses the critical G_c.

The specific evolution process of shear-crack features can be demonstrated below. Firstly, the plastic deformation accumulates gradually along the aforementioned shear plane with the advance of cutting edge, which causes the accumulation of potential energy for crack failure in the first deformation zone. Once the accumulated energy is large enough to overcome the fracture toughness, the initial cracks would be generated and are prone to propagate along the shear plane, as shown in Fig. 6b.

This material removal process (e.g., chip formation) can be interpreted from the view of energy equilibrium. When the cutter goes ahead a distance, dx_c, the total external energy supplied by cutting forces, ($U_{exter} = \int F_c dx$), are dissipated within forms of shear deformation energy consumed along the shear plane (U_{shear}), and frictional energy dissipated along the too-workpiece interface (U_{frict}), and potential energy for fracture propagation (U_{fract}) [31]. The detailed energy balance is now:

$$U_{exter} = U_{shear} + U_{frict} + U_{fract} \tag{2}$$

As seen from Eq. 1, the potential energy dissipated in the fracture process can be rewritten as

$$U_{fract} = \int G{\cdot}wdl \tag{3}$$

And the shear deformation energy can be regarded as the work done by shear force (F_s) within the movement (dx_s) along shear plane:

$$U_{shear} = \int F_s dx_s \tag{4}$$

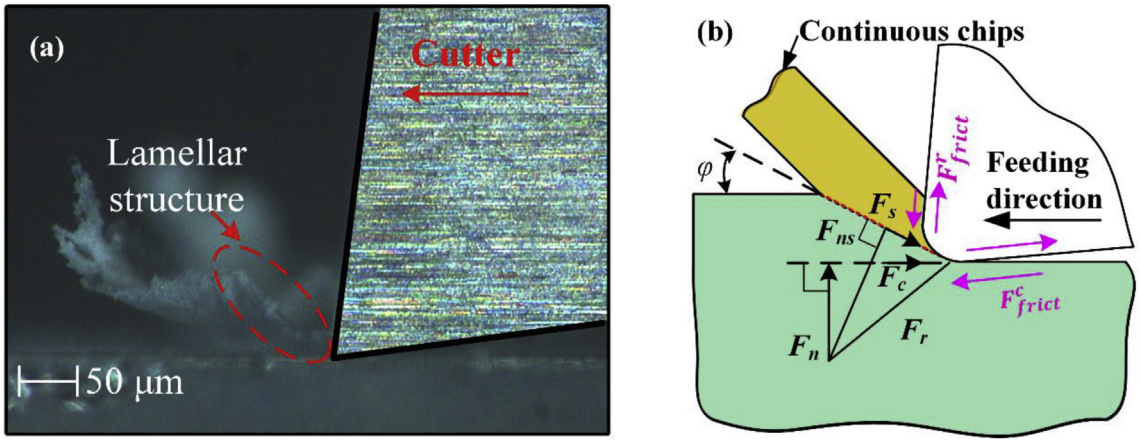

Fig. 5. Plastic cutting mode of KDP orthogonal cutting: (a) the continuous chips; (b) schematic of chip formation behaviour.

According to Merchant's analysis [26], the shear cutting force is given by:

$$F_s = \frac{\tau_s wh}{\sin\varphi} \tag{5}$$

where τ_s is the shear stress of KDP crystals in shear-crack cutting mode; w, h are the cutting width and UCT in these cutting tests, respectively. The term φ is the shear plane angle and can be defined as $2\varphi + \beta - \gamma_e = \frac{\pi}{2}$ according to Ernst-Merchant model where γ_e and β are the equivalent rake angle and friction angle, respectively.

Specifically, the friction angle (β) and shear strength (τ_s) in this case can be estimated by analysing the experimental data based on Merchant's analysis [26].

$$\tau_s = \frac{F_c\cos\varphi - F_n\sin\varphi}{wh/\sin\varphi} \tag{6}$$

$$\beta = \tan\mu = \tan\frac{F_c\tan\gamma_e + F_n}{F_c - F_n\tan\gamma_e} \tag{7}$$

It is worthy that, in the micromachining process, since the UCT decreases to the size of cutting edge radius (r_e), the instantaneous equivalent rake angle can not be regarded to equal to the nominal rake angle (γ) of the cutter. The equivalent rake angle is given by [32].

$$\gamma_e = \begin{cases} \sin^{-1}\left(\frac{h}{r_e} - 1\right), & h < r_e(1-\sin\gamma) \\ \gamma, & h \geq r_e(1-\sin\gamma) \end{cases} \tag{8}$$

In the shear plane, the instantaneous displacement (dx_s) of one unit chip driven by shear force can be expressed as:

$$dx_s = \frac{dx_c}{\cos\varphi} = \frac{v_c d_t}{\cos\varphi} \tag{9}$$

where dx_c presents the displacement of the cutter along the cutting direction. The terms dt and v_c donate the unit time and cutting speed in this cutting process, respectively.

The frictional work dissipated on the too-workpiece interface consists of two parts: the friction energy dissipated at the rake face of the cutter, U^r_{frict}, and that at clearance face, U^c_{frict}. The components of friction cutting forces at these two faces are given by

$$F^r_{frict} = \mu(F_c\cos(\gamma_e) - F_n\sin\gamma_e) \tag{10}$$

$$F^c_{frict} = \mu(F_n\cos(\varnothing) - F_c\sin\varnothing) \tag{11}$$

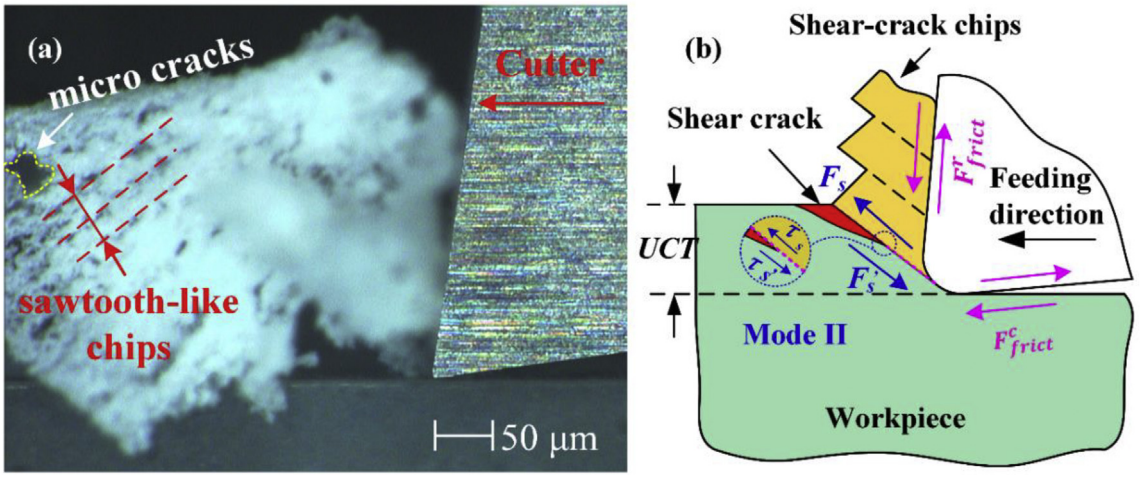

Fig. 6. Shear-crack cutting behaviour in KDP cutting: (a) shear-crack chips; (b) schematic of chip formation behaviour.

Based on the above analysis, the energy balance can be rewritten as

$$\int F_c dx = \int \frac{\tau_s wh}{\sin\varphi} dx_s + \int F^r_{frict} \cos(\gamma_e) dx + \int F^c_{frict} \cos(\varnothing) dx + \int G{\cdot}wdl \quad (12)$$

where the crack length dl can be assumed to equal to the cutting distance dx_c as it has been identified to be highly related to the movement of the cutter in a stable shear-crack cutting mode [33].

Therefore, the model for calculating the energy release rate for evaluating the chip formation process in shear-crack cutting mode can be expressed as

$$G = \frac{F_c}{w} - \frac{F^r_{frict}\cos(\gamma_e)}{w} - \frac{F^c_{frict}\cos(\varnothing)}{w} - \frac{\tau_s h}{\sin\varphi\cos\varphi} \quad (13)$$

3.2.3. Analysis of the brittle fracture chip formation in fracture cutting (FC) mode

In shear-crack cutting mode, the G in Mode II (Shearing) surpasses the shear fracture toughness of KDP crystals, increasing the risk of the generation of shear-cracks, while in the feed-rate direction this value is not big enough to bring about the initiation and propagation of large-size fractures [10]. However, with the further rise of UCT, both cutting and normal forces increase accordingly and would have an increasing role in dominating the material removal behaviour. When the G in feed-rate direction exceeds the critical G_c under mixed cutting load, the fracture cutting mode would come into being. This means that the chip formation process in fracture cutting mode is mainly dominated by the combination of Mode I: Opening and Mode II: Shearing, as shown in Fig. 7, with a feature of disconnected and powder chips.

The external cutting forces facilitating energy dissipations along feed-rate direction can be expressed as cutting (F_c) and normal (F_n) forces, which are given by [26]:

$$F_c = F_{ss}\cos(\beta-\gamma)/\cos(\varphi+\beta-\gamma) \quad (14)$$

$$F_n = F_{ss}\sin(\beta-\gamma)/\cos(\varphi+\beta-\gamma) \quad (15)$$

where F_{ss} is the shear force used for fracture cutting and can be evaluated as the difference of total shear force (F_s) minus the shear force (F_{sc}) used for generating shear-cracks, e. g., $F_{ss} = F_s - F_{sc}$, and the F_{sc} can be estimated as $F_{sc} = G_{IIc} \times w$.

Meanwhile, the instantaneous displacements (dx_n) corresponding to normal force (F_n) can be expressed as

$$dx_n = dx_s \sin\varphi = \tan\varphi v_c dt \quad (16)$$

Thus, the total work done by cutting and normal forces can be calculated as

$$U_c = \int F_c dx_c = \frac{(\tau_s h - G_{IIc}\sin\varphi) w\cos(\beta-\gamma_e) v_c dt}{\sin\varphi\cos(\varphi+\beta-\gamma_e)} \quad (17)$$

$$U_n = \int F_n dx_n = \frac{(\tau_s h - G_{IIc}\sin\varphi) w\sin(\varphi-\gamma_e)\tan\varphi v_c dt}{\sin\varphi\cos(\varphi+\beta-\gamma_e)} \quad (18)$$

where the G_{IIc} is the critical G contributed by shearing loads in the form of Model II, and can be expressed as

$$G_{IIc} = K^2_{IIc}/E \quad (19)$$

where the K_{IIc} can be estimated 1.2 times K_{Ic} ($K_{IIc} = 1.20K_{Ic}$) according to the analysis of Awaji et al., [34]; E is the elastic modulus of KDP crystals.

From the perspective of energy equilibrium, this total work (U_{exter}) supplied by the external cutting forces is not only dissipated in the fracture generation and propagation process but also consumed in frictional work. Considering the disconnected and powder-like chips, as shown in Fig. 3e-f, the friction work at the rake face of the cutter, U^r_{frict}, could be negligible; and thus, the frictional energy mainly includes the friction work dissipated at clearance face, U^c_{frict}. Therefore, the energy balance in this cutting mode is now:

$$\int F_c dx_c + \int F_n dx_n = \int F^c_{frict}\cos(\varnothing) dx + \int G{\cdot}wdl \quad (20)$$

Thus, substituting Eq. 17 and 18, the ultimate energy release rate for evaluating the material removal process in fracture cutting mode can be expressed as

$$G = \frac{(\tau_s h - G_{IIc}\sin\varphi)(\cos(\beta-\gamma_e) + (\sin(\beta-\gamma_e)\tan\varphi))}{\sin\varphi\cos(\varphi+\beta-\gamma_e)} - \frac{F^c_{frict}\cos(\varnothing)}{w} \quad (21)$$

4. Model verification and discussion on the proposed cutting modes

4.1. Validating the proposed model for the transition of cutting modes

As observed in Sec. 2.2, the evolution of cutting modes (e.g., PC, SCC, FC) in KDP cutting is highly related to the uncut chip thicknesses adopted in the cutting tests, which has been identified as a critical

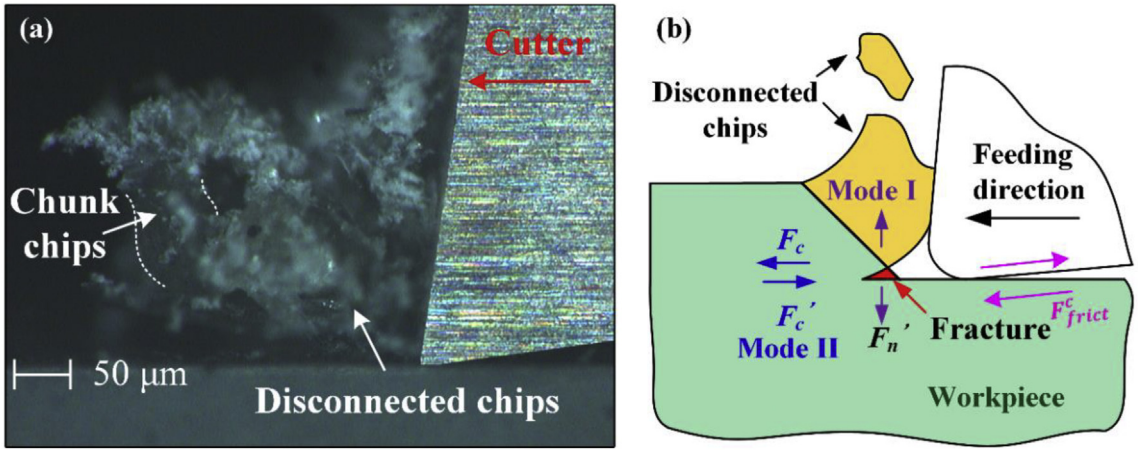

Fig. 7. Fracture cutting mode of KDP orthogonal cutting: (a) the fracture chips; (b) schematic of chip formation behaviour.

Table 2
Material property of single-crystal KDP on Double Plane.

Mechanical Properties		Values
Poisson's ratio υ		0.24 [35]
Elastic modulus E (Gpa)		40.89 [2]
Fracture toughness (MPa·m$^{1/2}$)	K_{Ic}	0.24 [35]
	K_{IIc}	1.20 · K_{Ic} [34]

parameter dominating the energy dissipation in chip formation processes. To validate this transition model, the specific mechanical properties of KDP crystals such as elastic modulus on the tested crystal plane are presented in Table. 2 and can be referred to existing works [35]. It is worthy to point out that the proposed models in Section 3 for calculating the G is partly based on the experimental results, especially the cutting forces at different UCT. According to Bifano's analysis [36], both the cutting forces and brittle-to-ductile transition of cutting behaviours are highly related to the mechanical properties of materials (i.e., elastic modulus, fracture toughness). Therefore, these material properties could have a potential influence on the calculated results of G by affecting the cutting forces.

Meanwhile, according to Merchant's theory where the orthogonal cutting process is in plane strain condition [26], the fracture criterion in FC mode can be estimated as the total critical G regarding mixed loading mode (Modes I/II) [30].

$$G_{(I+II)c} = \frac{K_{Ic}{}^2 + K_{IIc}{}^2}{E/(1-\vartheta^2)} \tag{22}$$

where K_{Ic} and K_{IIc} are the critical stress strength of KDP crystals in mode I and II. The terms v and E denote Poisson's ratio and elastic modulus of KDP crystals, respectively.

In KDP orthogonal cutting, the practical G in the shear-crack cutting mode is highly related to the brittle crack failure in mode II (Shearing Mode) and can be obtained using Eq. 13. The calculated G under varying UCT is presented in Fig. 8a. In shear-crack cutting mode, the energy release rate at different UCT has a similar magnitude although there is a slight fluctuation. For instance, the G in the case of cutting with a UCT = 1.25 μm is about 1948 N/m, a little larger than the critical value (G_{IIc} = 1885 N/m) for crack propagation. Subsequently, brittle crack failure would come into being in the formation process of chips, posing great rise of the generating shear-crack chips as aforementioned. While for the energy release rate in FC mode, a nearly constant stage can be observed with a moderate fluctuation as shown in Fig. 8b. The criteria for mixed modes I/II of brittle fractures is also presented. It is worthy to note that in some case (i.e., UCT = 12 μm), the calculated energy released rate is little lower than the critical value. This can be attributed to the nanoscale bulk defects and other irregularities inside KDP crystals [37], which were introduced in the crystal growth process and could weaken material strength and further exacerbate the fracture propagation when at mixed-mode cutting loads [38]. Besides, one can see that there is a statistical error for each calculated G in both cutting modes. These errors might occur due to the averaging of different material properties and also the experimental data (e.g. E, F_c) used in this work.

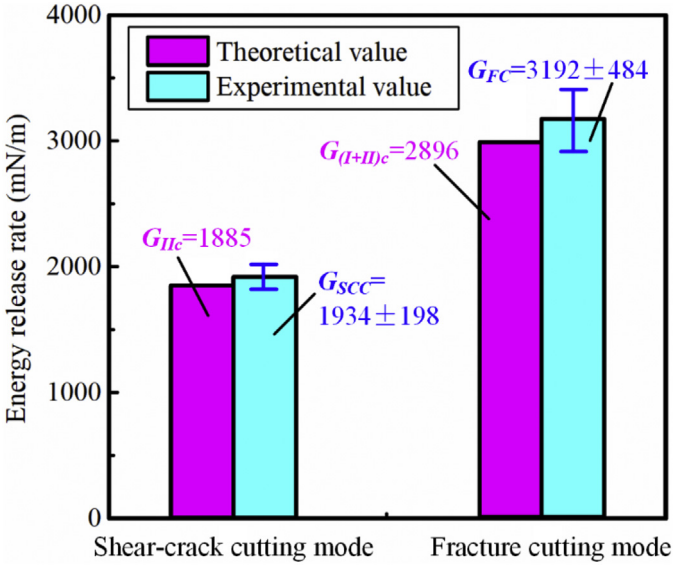

Fig. 9. Comparison of the average energy release rate in both shear-crack and fracture cutting modes.

Fig. 9 displays the comparison of the calculated G values between the experimental results (from Eq. 13 and 21) and theoretical analysis (from Eq.19 and 22) within shear-crack and fracture cutting modes. Overall, it can be concluded for the orthogonal cutting of soft-brittle KDP crystals:

$$G_{SCC} > G_{IIc}, G_{FC} > G_{(I+II)c}, \tag{23}$$

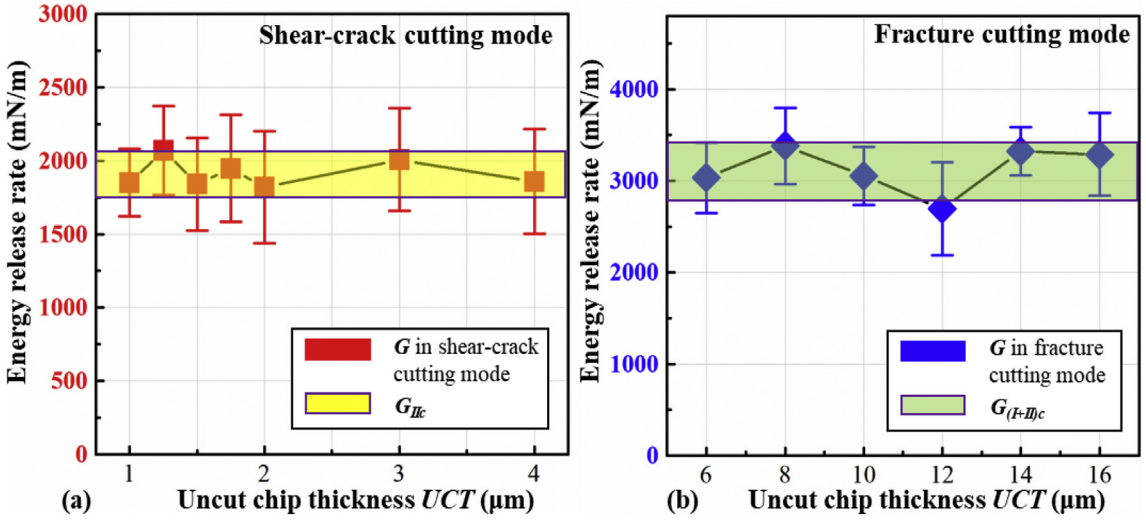

Fig. 8. The calculated mean values of G at different UCTs: (a) shear-crack cutting mode; (b) fracture cutting mode.

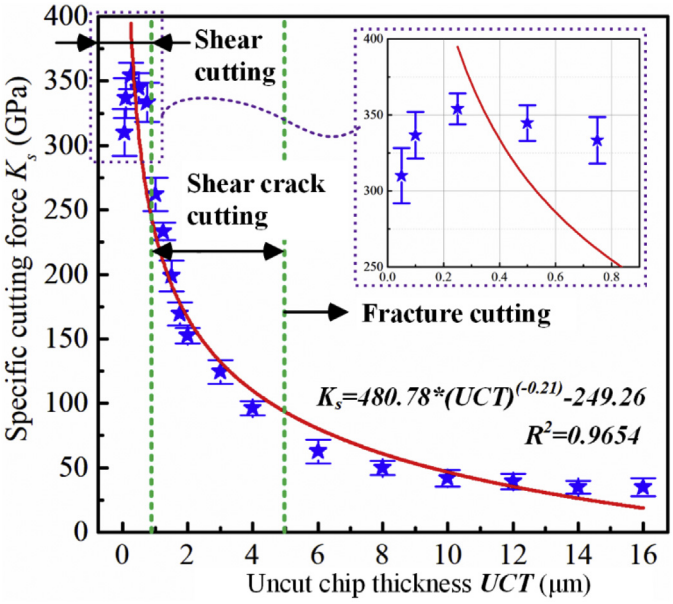

Fig. 10. The specific cutting forces at varying uncut chip thicknesses.

This clarifies that the G_{Fc} (3192 ± 484 mN/m) in fracture cutting condition exceeds that for critical mixed-loading modes ($G_{(I+II)c}$ = 2896 mN/m), while in shear-crack cutting condition the corresponding G_{SCC} (1934 ± 198 mN/m) surpasses the critical value (G_{IIc} = 1885 mN/m) for shear-cracks; therefore, brittle fracture and shear-crack chips were brought about in corresponding cutting conditions. These presented experimental and theoretical results well explained the formation mechanism of different chips (e.g. continuous, shear-crack and fracture chips) occurred in KDP cutting from the perspective of fracture mechanics and will facilitate the investigation of the material removal behaviour of soft-brittle KDP crystals for the next-step micromachining repair of KDP optical components.

4.2. Analysis of cutting forces within different cutting modes

Specific cutting force (K_s) is a key indicator to investigate the energy consumption state during cutting processes; and hence, it can be utilized to interpret the chip formation behaviours in KDP orthogonal cutting as the material removal (e.g., chip formation) is essentially an energy consumption process. The K_s can be expressed as:

$$K_s = \frac{F_c}{A_c} \tag{24}$$

where F_c and A_c are the average value of cutting forces and the cross-section area of UCT, respectively.

Therefore, the evolution of different material removal behaviours at different UCT can also be reflected by the specific cutting force calculated from the practical experimental data. Fig. 10 depicts the evolution of the specific cutting force with the varying UCT. One can see that with the rise of UCT, the K_s decreases dramatically at the lower range and tends to be stable at the higher range. This phenomenon on one hand can be attributed to the size effect of ploughing force [24], which will account for a larger proportion of the total cutting force when the UCT

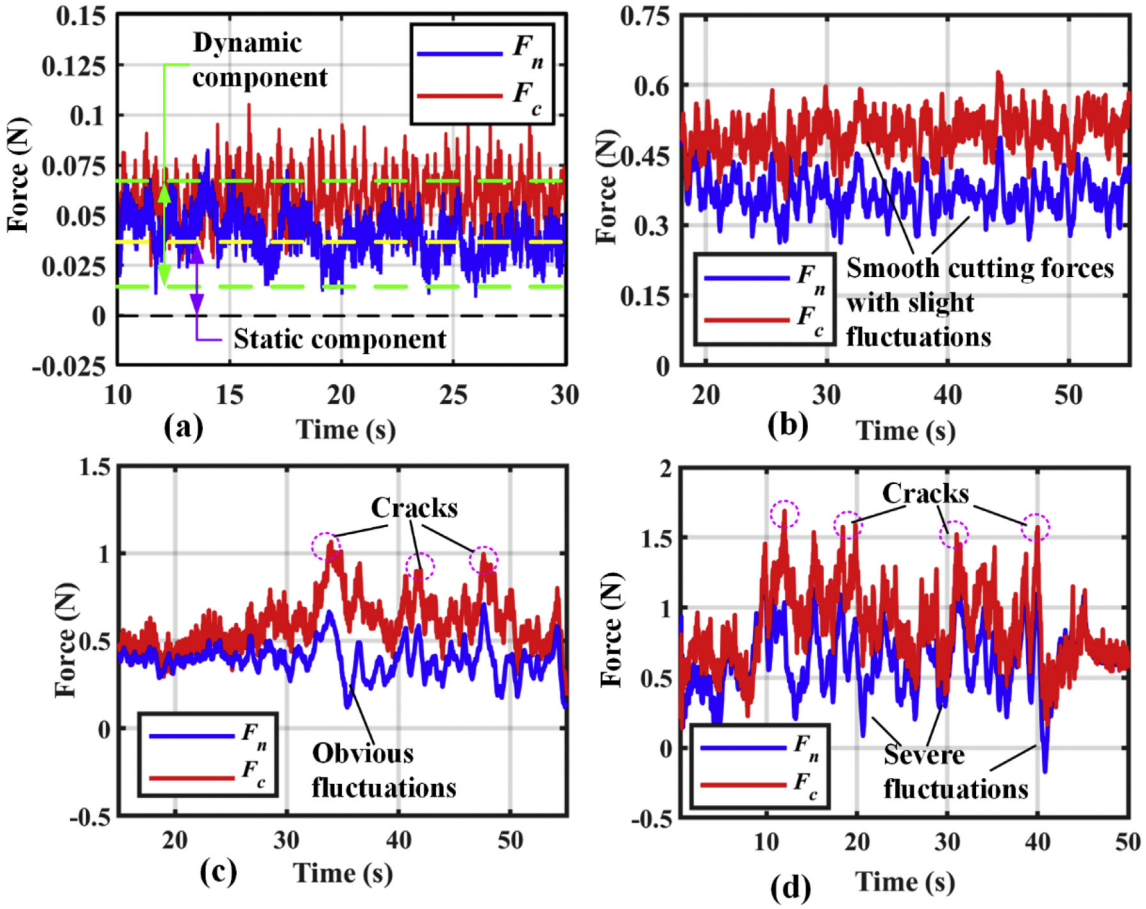

Fig. 11. Different cutting forces at varying UCTs: (a) 100 nm; (b) 750 nm; (3) 2 μm; (4) 8 μm.

decreases into nanoscale. On the other hand, the specific cutting force is also affected by the practical material removal behaviour. In plastic cutting mode within nano/sub-micro UCT, the whole ductile-regime cutting process requires a great number of unit energy consumption as the material removal is mainly dominated by plastic flow deformation. While with the increase of UCT, this specific cutting force witnesses a dramatic decrease in shear-crack cutting mode due to the crack propagation. Moreover, with the further increase of UCT, brittle fracture occurs and gradually dominates the material removal process in fracture cutting mode, causing the K_s decreases slightly and tends to be stable. From the perspective of specific cutting force, it can be concluded that increasing the UCT is conducive to reduce the energy consumption and improve the machinability of KDP crystals, but it has to pay the price for brittle material removal in forms of crack and fracture propagation and could result in worse surface integrity as the foregoing observations.

Fig. 11 shows the real-time cutting forces at different UCT which are extracted from the steady cutting stage and do not include the stages of tool input and output from workpieces as the cutting forces in these two stages (input and output) are not stable and highly influenced by the contact between the cutter and workpiece [39]. Meanwhile, to better understand the dynamic characteristic (i.e. crack generations) of cutting processes, the ratio of the dynamic component to mean value (static component, as annotated in Fig. 11a) of cutting forces at different UCTs was presented in Fig. 12. One can see that both of the cutting forces in plastic cutting mode (Fig. 11a and b) are companied by gentle fluctuations and the related ratios in Fig. 12 are less than 70%, close to that in metal cutting [26]. However, it is worthy to note that although both of them (Fig. 11a and b) are in plastic cutting mode, the ratio of cutting forces with a UCT of 100 nm in Fig. 12 is a bit higher than that in the case of UCT =750 nm. This indicates that a few of micro cracks may occur in the cutting process (UCT = 100 nm) although the entire material removal is mainly dominated by plastic shear deformation, which could be validated by the following surface morphology observation. The occurrence of these cracks could be attributed to the ploughing effect [24] as the magnitude of the adopted UCT is quite less than the radius value of the practical cutting edge.

While in shear-crack cutting mode (Fig. 11c), the fluctuation frequency and magnitude of the cutting forces show an increasing trend. This phenomenon can also be evidenced by the surging growth of the calculated ratio with the increase of UCT as shown in Fig. 12 and should be attributed to the generation and propagation of shear-cracks during the cutting process [40], which are normally accompanied with severe fluctuations of cutting forces [39]. When it comes to the fracture cutting mode, both the cutting force and the normal force in Fig. 11d fluctuate severely and even drop to zero-value sometimes, indicating the occurrence of brittle crack/fracture failure. This type of material removal behaviour ultimately brings the related ratio into a stable state with slight fluctuations (Fig. 12).

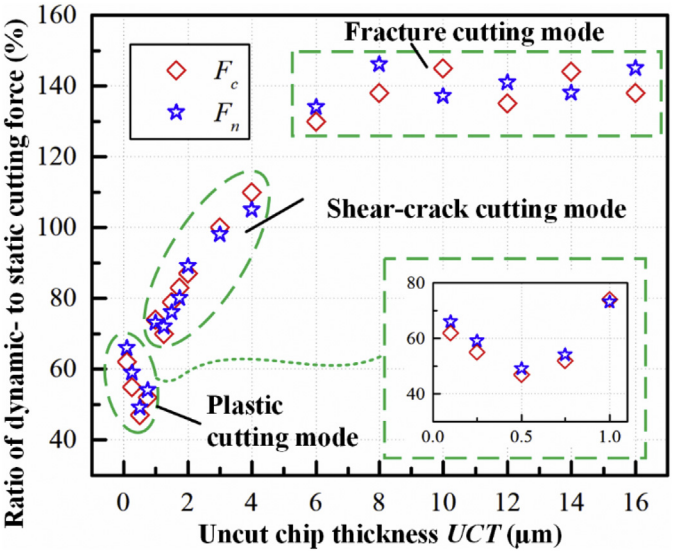

Fig. 12. The ratio of the dynamic component to mean value of cutting forces at different uncut chip thicknesses.

4.3. Surface morphologies machined at various cutting modes

Owing to the transitions of cutting behaviour/mode, the machined surface morphology in soft-brittle KDP cutting would be accordingly changed. The images of the representative surface morphologies machined at four different UCTs are presented in Fig. 13. The surface machined at UCT = 100 nm (Fig. 13a) was featured with many micro craters and micro pits while the surface machined under UCT = 750 nm (Fig. 13b) was nearly smooth with a few micro pits. This observation is opposite to the existing findings in the SPDT (cutting edge radius r_e≈40 nm) of soft-brittle KDP crystals [7], where the smaller is the UCT the better the quality of the machined surface can be. However, this finding coincides well with the results in micro ball-end milling of KDP crystals where a relatively large-radius cutting edge (r_e≈1.09 μm) was adopted [6]. As aforementioned, the radius of the cutting edge used in this work is about 1.118 μm, therefore, the practical UCT = 100 nm in Fig. 13a is far smaller than the cutting edge radius, resulting in severe ploughing behaviour [8,41]. In this case, the material underneath the cutting edge would undergo a mass of tensile stress, and owing to the soft-brittle nature of KDP crystals, the surface defects inevitable occurred on the machined surfaces. However, when the UCT/ r_e ratio in this cutting condition becomes higher than the critical value (UCT/ $r_e \approx 0.14$) of the ploughing effect for soft-brittle materials [23] the machined surface shows a much better quality, as shown Fig. 13b. This is because the material underwent substantial shear deformation and was removed with continuous chips, leaving a nearly smooth surface with a reduced level of defects than that shown in Fig. 13a. Moreover, in shear-crack cutting mode, a great number of micro craters were observed on the machined surface (UCT = 2 μm) as result of the generation of shear-cracks in the cutting process (Fig. 13c). Furthermore, in fracture cutting mode, the surface damage machined at UCT = 14 μm is much in evidence, as shown in Fig. 13d. Besides a few of ductile cutting trenches, a large edge-chipping removal was observed on the machined surfaces. This phenomenon resulted from the peeling up of conchoidal fracture after its initiation with the advance of the cutting tool. These damage features on the machined surfaces consist well with the previous observation of chip formations and the analysis of cutting forces, indicating that the generation mechanism of surface defects is also highly close to the UCT.

For the purpose of revealing the formation mechanism of surface defects, detailed morphologies of the aforementioned three types of surface defects are presented in Fig. 14. As seen in the magnified images (Fig. 14b-c), the dimension of micro pits along cutting direction was found to be a bit smaller than that perpendicular to cutting direction, making the majority of micro pits in an arc-shape. These micro pits were mainly generated by the material tearing after the passes of the cutter. Fig. 15a illustrates the detailed formation process of micro pits. In the practical cutting process, the material which is ahead of the cutter and also below the segment point, cannot be removed by forming chips. Instead, the material in this zone suffers from massive elastic-plastic deformation and tends to move downhill, resulting in one deformation layer underneath the cutter. After the cutter passes through it, this layer tends to spring back [42]. Meanwhile, due to the higher brittleness of KDP crystals, cracks are inevitable initiated by elastic recovery and propagate along the cleavage plane, resulting in the generation of micro pits, as illustrated in Fig. 15a.

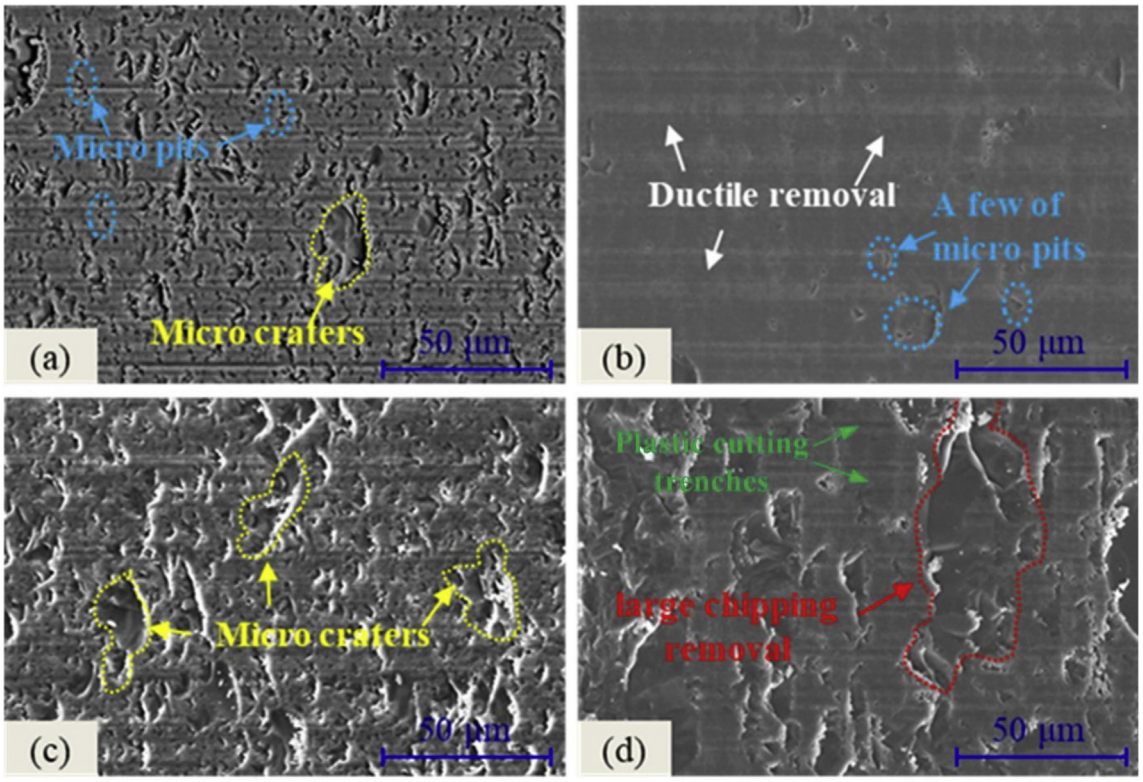

Fig. 13. SEM images for surface morphologies machined at different uncut chip thicknesses (UCT): (a) UCT = 100 nm; (b) UCT = 750 nm; (3) UCT = 2 μm; (4) UCT = 14 μm.

In regarding to micro craters, a step-like morphology can be observed on the machined surfaces (Fig. 14b). The generation of this step-like feature can be attributed to the crack initiation and its propagation motivated by the ploughing rub forces, as shown in Fig. 15b. With the advance of the cutting tool, these cracks propagate along different cleavage planes and may intersect each other until these damaged materials break away from the substrate, bringing about the formation of micro craters with step-like structures [40]. When it comes to the large-size edge chipping, a conchoidal fracture can be observed with a smoothly curving surface (Fig. 14c). As the previous discussion on the chip formation (Fig. 3f) and cutting force (Fig. 11d) at UCT = 14 μm, brittle fracture behaviour engages into the material removal process due to energy release rate exceeds its critical value for fracture propagation. As a consequence, a flake of KDP material is peeled

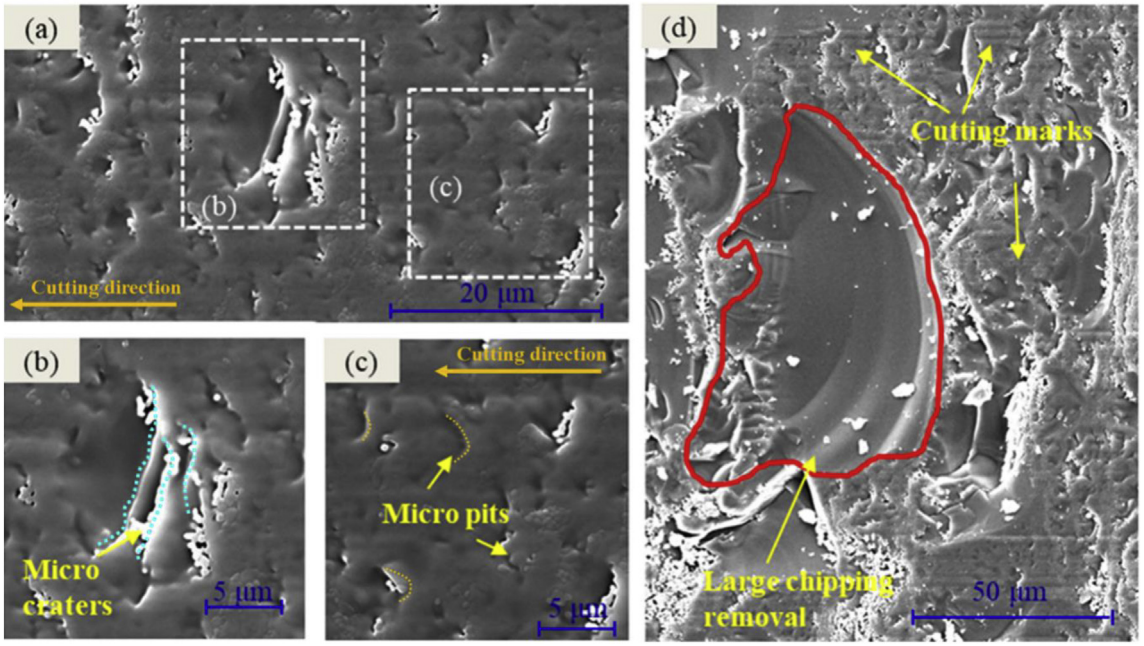

Fig. 14. The typical surface defects occurred on the machined KDP surface (a); Magnified images of micro craters (b) and micro pits (c); (d) shows the brittle large edge chipping fractures.

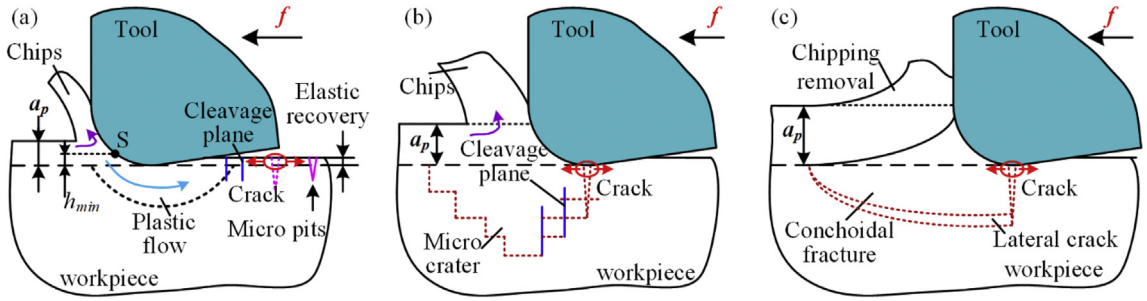

Fig. 15. The formation mechanism of three types of surface defects formed in KDP orthogonal cutting tests: (a) micro pits due to the tearing and spalling; (b) micro craters due to the ploughing effect; (c) edge-chipping removal due to the brittle fracture.

away, leaving the machined surface with a smoothly curving fracture feature (Fig. 15c).

Based on the above observation and analysis, the formation mechanism of surface defects with a relatively large-radius cutting edge ($r_e > 1$ μm) is different from that in SPDT of KDP crystals where a sharp edge is applied ($r_e < 0.1$ μm). Normally, in SPDT of brittle materials, one of prerequisite for ductile-regime cutting is to ensure the maximum value of *UCT* in practical cutting processes smaller than the critical value (UCT_c) of BDT. However, it was revealed here that, besides the upper limit (UCT_c), a lower limit for uncut chip thickness (UCT_l) must be taken into account due to the ploughing effect when adopting large-radius edges to machine soft-brittle materials, such as the micro ball-end milling of KDP crystals [43]. This means, in order to avoid micro craters and pits, the UCT should be in a reasonable range ($UCT_l < \mathrm{UCT} < UCT_c$) during the entire micromachining process, thereby guaranteeing the machining quality and efficiency of soft-brittle materials.

5. Conclusion

Micromachining with a relatively large-radius cutting edge is a promising and economical method for repairing the surface defects on KDP optics; and thus, understanding the corresponding material removal mechanism is of great importance. This paper aims to study the chip formation behaviours and surface-defect generation in KDP orthogonal cutting processes. Three different cutting modes were observed based on the observation of chip morphologies. The energy release rate consumed in chip formation processes was innovatively modelled to explain the different material cutting behaviours with varying uncut chip thickness and was validated well with the cutting forces and machined surface morphologies. While this work might not be able to decipher all unsolved phenomena occurred in practical micromachining of KDP optical components like the anisotropy of cutting direction, it is supposed to present an initial understanding on the material removal response in cutting soft-brittle materials with a relatively large-radius cutting edge.

In KDP orthogonal cutting, the chip morphologies display three types of features (e.g., continuous, shear-crack, fracture chips) when increasing the uncut chip thickness (UCT); and therefore, by referring to UCT, the material removal mechanism can be divided into three modes: plastic cutting (PC), shear-crack cutting (SCC) and fracture cutting (FC) modes. An analytical model has been proposed for calculating the energy release rate within different cutting modes. It is revealed that from the perspective of fracture mechanic the specific material removal behaviour in KDP orthogonal cutting is dominated by the energy release rate in the chip formation process. The experimental results consist well with the theoretical analysis, validating the proposed theoretical approach for understanding the ductile-regime cutting mechanism of soft-brittle solids. Meanwhile, the specific cutting force is found to be higher in PC mode within nano/micro UCT but then shows a substantial decreasing trend with the arise of UCT in SCC mode followed by a lower-value and stable stage in FC mode. The brittle crack/fracture failure can also be reflected the average ratio of the dynamic component to the mean value of cutting forces, which tends to increase with the generation of cracks and even exceeds 100% when large-size fractures occur. Besides, three types of surface defects (e.g., micro pits, micro craters, large-size edge chipping) are observed on machined surfaces with different generation mechanism. These three kinds of surface defects were caused by tearing and spalling of materials with elastic recovery, crack propagation along cleavage planes with ploughing effect, and the peeling away of large-size fractures, respectively.

This research reveals that a lower limit for uncut chip thickness must be taken into account when adopting relatively large-radius cutting edge for micromachining repair of soft-brittle KDP optics due to the ploughing effect. This means, in order to avoid micro craters and pits, the UCT should be chosen in a reasonable range during the entire micromachining process, thereby guaranteeing the machining quality and efficiency of soft-brittle materials. This can also support the future design of the machining strategy of KDP single-crystals and other soft-brittle materials as well as their cutting tool development.

Credit author statement

Qi Liao: Conceptualization; Methodology; Investigation; Formal analysis; Writing- Original draft preparation, editing.

Zhirong Liao: Conceptualization; Methodology; Investigation; Formal analysis; Supervision; Review & Editing; Supervision; Resources; Funding acquisition.

Jian Cheng: Resources; Reviewing and Editing;

Dongdong Xu: Methodology; Reviewing and Editing;

Mingjun Chen: Resources; Supervision; Reviewing and Editing; Funding acquisition.

Declaration of Competing Interest

The authors declare that they have no known competing financial interests or personal relationships that could have appeared to influence the work reported in this paper.

Acknowledgement

This research is supported by the National Key Research and Development Program of China (No. 2017YFB0305900), National Natural Science Foundation of China (No. 51775147, 51705105), Science Challenge Project (No. TZ2016006-0503-01), Young Elite Scientists Sponsorship Program by CAST (No. 2018QNRC001), China Postdoctoral Science Foundation (Nos. 2017M621260, 2018T110288) and Self-Planned Task (Nos. SKLRS201803B, SKLRS201718A) of State Key Laboratory of Robotics and System (HIT). The authors also appreciate the support from Nottingham research fellowship programme.

References

[1] J. Cheng, Y. Xiao, Q. Liu, H. Yang, L. Zhao, M. Chen, J. Tan, W. Liao, J. Chen, X. Yuan, Effect of surface scallop tool marks generated in micro-milling repairing process on the optical performance of potassium dihydrogen phosphate crystal, Mater. Des. 157 (2018) 447–456.

[2] Q. Liu, Z. Liao, D. Axinte, Temperature effect on the material removal mechanism of soft-brittle crystals at nano/micron scale, Int J Mach Tool Manu (2020), https://doi.org/10.1016/j.ijmachtools.2020.103620.

[3] H. Yang, J. Cheng, Z. Liu, Q. Liu, L. Zhao, J. Wang, M. Chen, Dynamic behavior modeling of laser-induced damage initiated by surface defects on KDP crystals under nanosecond laser irradiation, Sci. Rep. 10 (1) (2020) 500.

[4] M. Chen, W. Ding, J. Cheng, H. Yang, Q. Liu, Recent Advances in Laser-Induced Surface Damage of KH2PO4 Crystal, Appl.Sci. 10 (19) (2020).

[5] H. Yang, J. Cheng, M. Chen, J. Wang, Z. Liu, C. An, Y. Zheng, K. Hu, Q. Liu, Optimization of morphological parameters for mitigation pits on rear KDP surface: experiments and numerical modeling, Opt. Express 25 (15) (2017) 18332–18345.

[6] Q. Liu, J. Cheng, Y. Xiao, M. Chen, H. Yang, J. Wang, Effect of tool inclination on surface quality of KDP crystal processed by micro ball-end milling, Int. J. Adv. Manufac. Tech. 99 (9) (2018) 2777–2788.

[7] S. Zhang, W. Zong, A novel surface roughness model for potassium dihydrogen phosphate (KDP) crystal in oblique diamond turning, Int. J. Mech. Sci. 173 (2020) 105462.

[8] Y.J. Lee, H. Wang, Current understanding of surface effects in microcutting, Mater. Des. 192 (2020) 108688.

[9] S. Wang, C. An, F. Zhang, J. Wang, X. Lei, J. Zhang, An experimental and theoretical investigation on the brittle ductile transition and cutting force anisotropy in cutting KDP crystal, Int J Mach Tool Manu 106 (2016) 98–108.

[10] Z. Liao, D.A. Axinte, On chip formation mechanism in orthogonal cutting of bone, Int J Mach Tool Manu 102 (2016) 41–55.

[11] S. Zhang, H. Zhang, W. Zong, Modeling and simulation on the effect of tool rake angle in diamond turning of KDP crystal, J. Mater. Process. Tech. 273 (2019) 116259.

[12] Q. Liu, J. Cheng, Y. Xiao, H. Yang, M. Chen, Effect of milling modes on surface integrity of KDP crystal processed by micro ball-end milling, Proc. CIRP 71 (2018) 260–266.

[13] N. Chen, L. Li, J. Wu, J. Qian, N. He, D. Reynaerts, Research on the ploughing force in micro milling of soft-brittle crystals, Int. J. Mech. Sci. 155 (2019) 315–322.

[14] S. Wojciechowski, M. Matuszak, B. Powałka, M. Madajewski, R.W. Maruda, G.M. Królczyk, Prediction of cutting forces during micro end milling considering chip thickness accumulation, Int J Mach Tool Manu 147 (2019).

[15] Y. Yuan, X. Jing, K.F. Ehmann, J. Cao, H. Li, D. Zhang, Modeling of cutting forces in micro end-milling, J. Manuf. Process. 31 (2018) 844–858.

[16] Q. Liu, J. Cheng, H. Yang, Y. Xu, L. Zhao, C. Tan, M. Chen, Modeling of residual tool mark formation and its influence on the optical performance of KH2PO4 optics repaired by micro-milling, Opt. Mater. Express 9 (9) (2019) 3789.

[17] T.G. Molnar, S. Berezvai, A.K. Kiss, D. Bachrathy, G. Stepan, Experimental investigation of dynamic chip formation in orthogonal cutting, Int J Mach Tool Manu 145 (2019).

[18] D. Xu, Z. Liao, D. Axinte, M. Hardy, A novel method to continuously map the surface integrity and cutting mechanism transition in various cutting conditions, Int. J. Mach. Tool Manufact. 151 (2020).

[19] B. Wang, Z. Liu, Evaluation on fracture locus of serrated chip generation with stress triaxiality in high speed machining of Ti6Al4V, Mater. Des. 98 (2016) 68–78.

[20] J.A. Robles-Linares, D. Axinte, Z. Liao, A. Gameros, Machining-induced thermal damage in cortical bone: Necrosis and micro-mechanical integrity, Mater. Des. 197 (2021).

[21] Z. Liao, A. Abdelhafeez, H. Li, Y. Yang, O.G. Diaz, D. Axinte, State-of-the-art of surface integrity in machining of metal matrix composites, Int J Mach Tool Manu 143 (2019) 63–91.

[22] O. Gavalda Diaz, G. Garcia Luna, Z. Liao, D. Axinte, The new challenges of machining ceramic matrix composites (CMCs): review of surface integrity, Int J Mach Tool Manu 139 (2019) 24–36.

[23] N. Chen, M. Chen, C. Wu, X. Pei, Cutting surface quality analysis in micro ball end-milling of KDP crystal considering size effect and minimum undeformed chip thickness, Precis. Eng. 50 (2017) 410–420.

[24] N. Chen, M. Chen, C. Wu, X. Pei, J. Qian, D. Reynaerts, Research in minimum undeformed chip thickness and size effect in micro end-milling of potassium dihydrogen phosphate crystal, Int. J. Mech. Sci. 134 (2017) 387–398.

[25] Z. Shi, Q. Zhao, B. Guo, T. Ji, H. Wang, A review on processing polycrystalline magnesium aluminate spinel (MgAl2O4): Sintering techniques, material properties and machinability, Mater. Des. 193 (2020).

[26] M.E. Merchant, Mechanics of the Metal Cutting Process. I. Orthogonal Cutting and a Type 2 Chip, J. Appl, Phys 16 (5) (1945) 267–275.

[27] D.A. Axinte, S. Abdul Shukor, A.T. Bozdana, An analysis of the functional capability of an in-house developed miniature 4-axis machine tool, Int J Mach Tool Manu 50 (2) (2010) 191–203.

[28] D. Xu, Z. Liao, D. Axinte, J.A. Sarasua, R. M'Saoubi, A. Wretland, Investigation of surface integrity in laser-assisted machining of nickel based superalloy, Mater. Des. 194 (2020).

[29] N. Hou, L. Zhang, Y. Zhang, F. Zhang, On the ultra-precision fabrication of damage-free optical KDP components: mechanisms and problems, Crit. Rev. Solid State Mater. Sci. (2018) 1–15.

[30] J. Chang, J.-q. Xu, Y. Mutoh, A general mixed-mode brittle fracture criterion for cracked materials, Eng. Fract. Mech. 73 (9) (2006) 1249–1263.

[31] Y. Patel, B.R.K. Blackman, J.G. Williams, Determining fracture toughness from cutting tests on polymers, Eng. Fract. Mech. 76 (18) (2009) 2711–2730.

[32] S. Venkatachalam, X. Li, S.Y. Liang, Predictive modeling of transition undeformed chip thickness in ductile-regime micro-machining of single crystal brittle materials, J. Mater. Process. Tech. 209 (7) (2009) 3306–3319.

[33] T. Atkins, Chapter 3 - simple orthogonal cutting of floppy, brittle and ductile materials, in: T. Atkins (Ed.), The Science and Engineering of Cutting, Butterworth-Heinemann, Oxford 2009, pp. 35–74.

[34] H. Awaji, T. Kato, S. Honda, T. Nishikawa, Criterion for combined mode I-II of brittle fracture, J. Ceram. Soc. Jpn. 107 (1250) (1999) 918–924.

[35] T. Fang, J.C. Lambropoulos, Microhardness and indentation fracture of potassium Dihydrogen phosphate (KDP), J. Am. Ceram. Soc. 85 (1) (2004) 174–178.

[36] T.G. Bifano, T.A. Dow, R.O. Scattergood, Ductile-regime grinding. A new technology for machining brittle materials, J. Eng. Ind. Trans. ASME 113 (2) (1991) 184–189.

[37] S.G. Demos, M. Staggs, H.B. Radousky, Bulk defect formations in KH_2PO_4 crystals investigated using fluorescence microscopy, Phys. Rev. B 67 (22) (2003) 224102.

[38] K. Liu, H. Wang, X. Zhang, Ductile mode cutting of tungsten carbide, in: K. Liu, H. Wang, X. Zhang (Eds.), Ductile Mode Cutting of Brittle Materials, Springer Singapore, Singapore, 2020.

[39] T. Matsumura, P. Aristimuno, E. Gandarias, P.J. Arrazola, Cutting process in glass peripheral milling, J. Mater. Process. Tech. 213 (9) (2013) 1523–1531.

[40] S. Goel, X. Luo, P. Comley, R.L. Reuben, A. Cox, Brittle–ductile transition during diamond turning of single crystal silicon carbide, Int J Mach Tool Manu 65 (2013) 15–21.

[41] M. Zhang, D. Zhang, D. Geng, J. Liu, Z. Shao, X. Jiang, Surface and sub-surface analysis of rotary ultrasonic elliptical end milling of Ti-6Al-4V, Mater. Des. 191 (2020) 108658.

[42] F.Z. Fang, H. Wu, W. Zhou, X.T. Hu, A study on mechanism of nano-cutting single crystal silicon, J. Mater. Process. Tech. 184 (1–3) (2007) 407–410.

[43] Q. Liu, J. Cheng, Z. Liao, H. Yang, L. Zhao, M. Chen, Incident laser modulation by tool marks on micro-milled KDP crystal surface: numerical simulation and experimental verification, Opt. Laser Technol. 119 (2019) 105610.